CrystEngComm

Accepted Manuscript

ROYAL SOCIETY OF CHEMISTRY

www.rsc.org/crystengcomm

Journal Name

ARTICLE

Received 00th January 20xx,
Accepted 00th January 20xx

DOI: 10.1039/x0xx00000x

www.rsc.org/

Propeller-shaped molecules with thiazole hub: structural landscape and hydrazone cap mediated tunable host behavior in 4-hydrazino-1,3-thiazoles

Sarah Titus and Kumaran G. Sreejalekshmi*

Propeller-shaped molecules with 2,4,5-trisubstituted-1,3-thiazole as hub and tunable blades (**B_1-B_3**) were synthesized as trivariant scaffolds. **B_1-B_3** were modulated by varying hydrazone capping in **B_1**, isothiocyanate in **B_2** and α-haloketone in **B_3** and the structural landscapes examined. Multicomponent molecular crystals formed nitrogen rich channels (NRC) of varying shapes and dimensions which were largely steered by substitution pattern in **B_1** and established by varying carbonyl components. Isopropylidene derivatives (IPHAT) stabilized single file water inside NRC (~34 $Å^2$) between **B_1** and **B_2**, benzylidene derivative (BzHAT) formed a constricted NRC and accommodated solvates inside a hydrophobic cavity between **B_1** and **B_3** whereas a pincer-shaped NRC devoid of guest molecules was formed by cyclohexylidene derivative (CyHAT). Hydrazone substituent-driven variation in solid state landscapes indicates wide scope of expandability in these thiazole templates as supramolecular synthons for tunable hosts.

Introduction

[a] *Department of Chemistry, Indian Institute of Space Science and Technology, Valiamala Post, Thiruvananthapuram – 695 547, India*

† Electronic Supplementary Information (ESI) available: CCDC reference numbers 1002352,1002353,1052981,1052982,1052983. See DOI: 10.1039/x0xx00000x

The implicit interdependency of crystal engineering and drug design is well assimilated given the significance of molecular interactions in both.[1, 2] The determination of crystal structures being imperative for drug design,[3, 4] development and formulations, identifies the role of molecular structure in crystal packing and its influence on physicochemical properties of the drug candidate.[5] Whereas drug design seek parent scaffolds that endorse molecular diversity[6-11] and are likely to afford crucial interactions (eg: intramolecular hydrogen bonds), similar considerations arise in the design of supramolecular synthons[12-15] for custom-made materials from first principles. For example, the correlation of intramolecular hydrogen bonding with improved membrane permeability[16] motivate drug designer to incorporate donor/acceptor sites in the chosen molecular fragments while a plethora of factors encourage a synthetic expert in supramolecular domain in doing so.[17-19] Our recent research focuses on design and synthesis of materials based on thiazole scaffolds for molecular therapeutics.[20-22] It is a well known fact that despite huge costs involved in the drug discovery process and largely static output in terms of launching new drugs,[23,24] a large number of molecular fragments bear the burden 'of no use' and get discarded.[25-27] Having mentioned the similar features in the design of drug and supramolecular synthon, and successful application of crystal engineering in pharmaceutics[28-32] we felt it worthy to investigate the solid state structures of novel 4-hydrazino-1,3-thiazoles[33] as supramolecular synthons, in an attempt to explore and expand its applicability in materials science along with its potential applications in drug discovery. In the present study we spotlight on the supramolecular assemblages and potentially tunable guest encapsulations in these propeller-shaped trivariant systems by varying the substituents at the hydrazono position (Fig. 1).

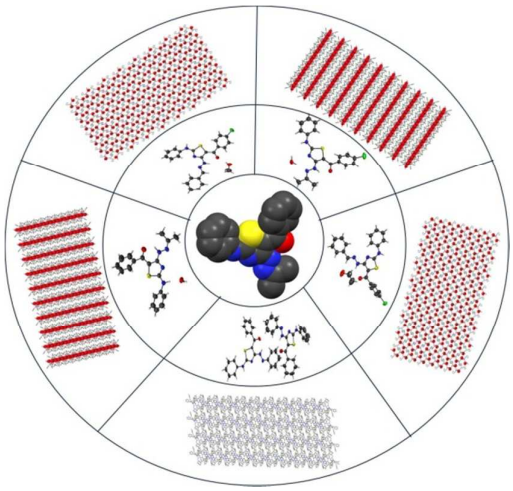

Fig. 1 Multicomponent molecular crystals of 4-hydrazinothiazoles as synthetic hosts.

Results and Discussion

The impetus for design of 4-alkylidene/arylidenehydrazino-5-(substituted)aroyl-2-(substituted)amino-1,3-thiazole (Fig. 2) stems from likely vast diversity multiplication and scaffold enrichment by varying carbonyl component, isothiocyanate or active methylene unit, thus making a trivariant system (Table 1). Furthermore, the parent scaffold encompasses a range of donor-acceptor groups with imbalances in their numbers, thus amenable to intra and intermolecular interactions and the formation of multicomponent crystals (hydrates/solvates)[34, 35] was also predicted. Geometry optimizations (6-31G basis set, Gaussian 09 program) indicated (Fig. S1) the molecules to adopt a propeller shape with a thiazole hub encased by three blades ($\mathbf{B_1}$-$\mathbf{B_3}$), and encouraged synthesis and studies of solid state landscapes in these novel systems.

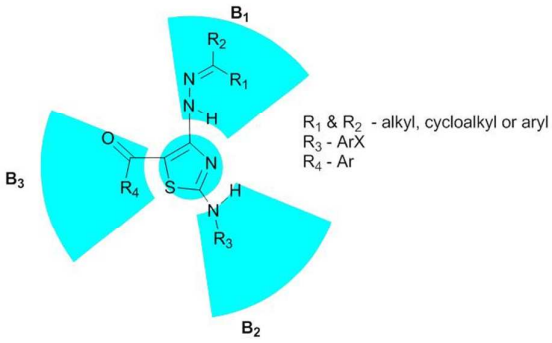

Fig.2 General structure of 4-hydrazino-5-aroyl-2-amino-1,3-thiazole.

Table 1 Variations in $\mathbf{B_1}$-$\mathbf{B_3}$.

Entry	R_1	R_2	R_3	R_4
IPHAT 1	$-CH_3$	$-CH_3$	$-C_6H_5$	$-C_6H_5$
IPHAT 2	$-CH_3$	$-CH_3$	$-C_6H5$	$4\text{-}ClC_6H_4$
BzHAT	$-C_6H_5$	-H	$-C_6H_5$	$4\text{-}ClC_6H_4$
CyHAT		$-C_6H_{10}-$	$-C_6H_5$	$-C_6H_5$

Modular synthesis of the molecules was achieved in a versatile sequential multicomponent reaction (SMCR) for [4+1] thiazole ring formation under mild conditions. In the present communication, focus is on providing variants at the hydrazone site by varying carbonyl components and to inspect their influence on the crystal landscape and possible supramolecular assemblages. Interestingly, while probing crystal structures, we found multicomponent molecular crystals from these novel systems to manifest as synthetic hosts for one dimensional (1D) water chains, polar protic solvents and in some cases to house unoccupied voids, all attributed to the variations in the carbonyl capping units employed for hydrazone formation implying tunable hosts.

1D water chains

One dimensional (1D) water chains/water wires and design of their synthetic hosts attract enormous research interest owing to their key roles in fundamental biological processes[36-39] exemplified by selective transport of water across cells in protein aquaporin,[40-45] transport of protons in Gramicidin A membrane channels,[46-50] cytochrome oxidase,[51-56] and bacteriorhodopsin.[57-59] The probable role of water in protein folding[60, 61] and correlation of water pathways to the activation of G-coupled receptors[62] all point towards the topical interest in water channels. Albeit the implicit significance of water pores, biomimetic design of synthetic water channels[63] kept low pace, except for a few complex architectures inspired by aquaporin water[64, 65] or influenza A proton channel[66, 67] till recently. Both inorganic and organic molecules have proven as host lattices for water in restricted environments. The huge potential of organic molecules, which have a tendency to crystallize as hydrate[68-74] and the factors stabilizing the hydrates[75] all provide cue to mimic natural systems among which urea based[76-78] or imidazole based,[79, 80] were demonstrated as functional channels for ions or water (protons) whereas calixpyrroles[81] were reported to stabilize 1D water chains. In yet another perspective, water in hydrates has been utilized as a design element in crystal engineering.[82, 83] Expanding the crystal database of organic hydrates further, we present the synthesis and structural landscapes in hitherto unexplored molecular crystals with a thiazole core. Providing acetone as the carbonyl capping for hydrazine unit in $\mathbf{B_1}$, we accomplished the synthesis of IPHAT 1 and IPHAT 2 as previously reported by our group.[33] Diffraction quality crystals were obtained by slow evaporation from aqueous ethanolic solutions. Both systems evolved as monohydrates belonging to non-centrosymmetric space group $P2_1/c$ with Z= 4 with packing coefficients of 0.680 (IPHAT 1) and 0.690 (IPHAT 2), whereby the basic building block appeared as a butterfly-shaped dimer (Fig. 3) formed by the antiperiplanar arrangement of thiazole rings pushing the C=O in $\mathbf{B_3}$ to the exterior and aligning $\mathbf{B_1}$ and $\mathbf{B_2}$ to accommodate the water molecules in between.

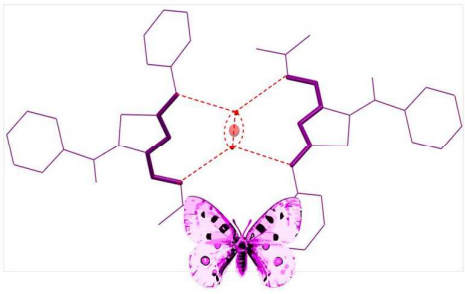

Fig. 3 Butterfly shaped dimer formed by IPHAT.

The H-bonding associations, as anticipated, followed Etters' rules[84] where both intra and intermolecular bonds were observed. H-bonding in IPHAT 1 and IPHAT 2 (viewed along *b* axis) indicate H-bond distances in the range of 2.61-2.89 Å (dD···A). The oxygen atom of each water molecule in IPHAT 1 and IPHAT 2 is simultaneously H-bonded to NH in $\mathbf{B_2}$ (dO···H 1.89 Å in IPHAT 1 and 2.06 Å in IPHAT 2) and to neighboring water molecules (dO···H 1.92 Å in IPHAT 1 and 1.96 Å in IPHAT 2) in a zig-zag manner. These H-bonded water molecules (dO–O 2.86 Å in IPHAT 1 and 2.85 Å in IPHAT 2) form infinite 1D water chains in the respective crystal lattice with O-O distances comparable to that observed in aquaporin water channels (2.8 Å)[43] (Fig. S2). Expanding the crystal landscape further, solid state assemblies indicated recurrent water chains (two per unit cell) separated by (interplanar distances) 9.097 Å in IPHAT 1 and 9.829 Å in IPHAT 2 (Fig. S3) and with opposite dipolar orientations (Fig. 4) as reported for the imidazole quartet.[76]

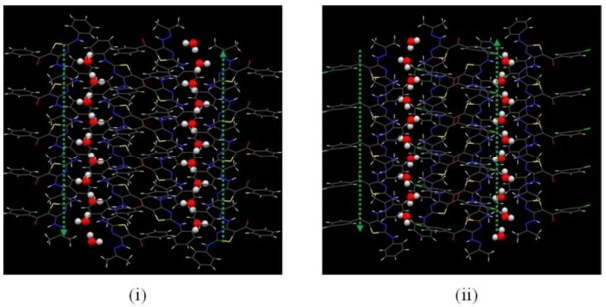

Fig. 4 Dipolar orientation of water channels (green arrow) in (i) IPHAT 1 and (ii) IPHAT 2. Water molecules are shown in ball and stick representation.

Planar arrangement of layered stacks with an inter layer distance of 4.854 Å are generated along *ac* plane such that thiazole hub and the phenyl rings on $\mathbf{B_2}$ and $\mathbf{B_3}$ (intercentroidal distances 4.956 Å and 4.854 Å in IPHAT 1 and IPHAT 2 respectively) are disposed at the extremities of a columnar structure contributing to the formation of a NRC resembling a left-handed helix which enclosed tetrahedral H-bonded water molecules as a single file (Fig. 5). The area enclosing water wire in the NRC was calculated and found to be ~34 $Å^2$ units in both IPHAT 1 and IPHAT 2 (Fig. S4).

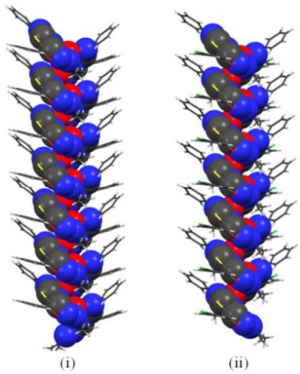

Fig. 5 View of N-rich left handed helix enclosing 1D water wire in (i) IPHAT 1 (ii) IPHAT 2 along *c* axis. All H atoms are omitted for clarity of view. NRC and oxygen atom of water molecule are in CPK representation.

It was interesting to note that H-bonding between water molecules and the NRC defined a graph set $R_3^3(10)$. The interlayer stabilizations from π- π stacking interactions between thiazole moieties, those between phenyl rings, along with the strong hydrophobic van der Waals interaction between the methyl groups in the isopropylidene unit, all are deemed to contribute to the formation and stabilization of water channel superstructures (Fig. 6). Apart from these intermolecular H-bonding, strong intramolecular H-bonding exists between the C=O in $\mathbf{B_3}$ and NH on $\mathbf{B_1}$, in a graph set *S(6)*, (dO···H 1.85 Å in IPHAT 1 and 1.91 Å in IPHAT

2 respectively) which synergistically contribute to the stability of these assemblies.

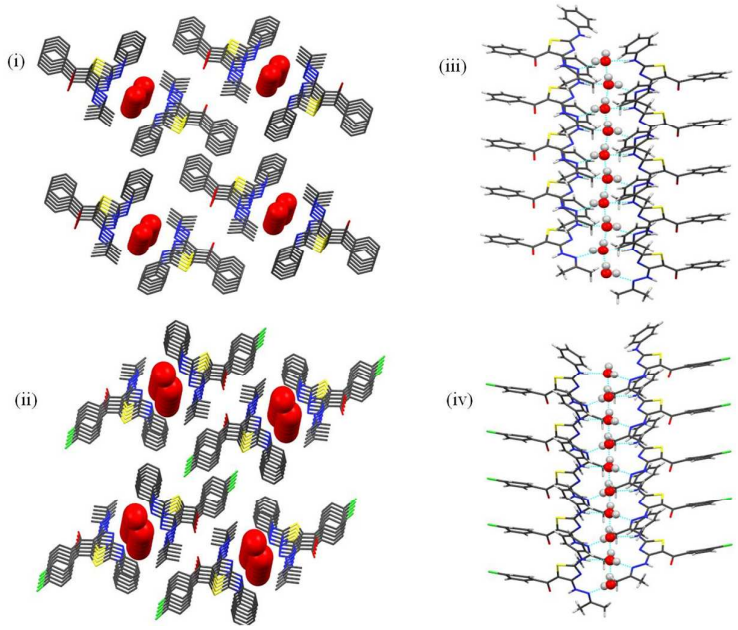

Fig. 6 View of packing diagram of (i) IPHAT 1 and (ii) IPHAT 2 in *ac* plane. Water molecules are CPK representation. All H atoms are omitted for clarity of view. Single file water chain (along *c* axis) in (iii) IPHAT 1 and (iv) IPHAT 2. Water molecules are shown in ball and stick representation.

The observed hydrophobic gateway formed by aryl ring in $\mathbf{B_2}$ and alkyl groups in $\mathbf{B_1}$ housing the water in a single file arrangement further may be correlated to hydrophobic gating in biological channels[85] and may be highly significant to regulate the flow of solvent/ions. We expect these unique molecular skeletons which assemble predominantly through H-bonding and π-π stacking to generate unique channels will serve as suitable starting points for the design and development of synthetic water channels based on thiazole core. The proton/ion transport properties of these molecules will be reported summarily.

Solvates (polar protic)

To expand the studies we next decided to focus on $\mathbf{B_1}$ variant for four reasons – i) the ease of access to carbonyl compounds so as to have diverse systems ii) to explore the critical role of hydrazone substituents on NRC dimensions iii) to probe the influence of hydrophobic linings in water channel formation and finally iv) to formulate guidelines regarding predictability of guest encapsulations and hence tunability of the channels. To that end we employed benzaldehyde as the carbonyl component and synthesized BzHAT and diffraction grade crystals were grown under previous conditions. While examining the crystal landscape, it was interesting to notice that hydrate formation was not preferred as with IPHAT derivatives and the NRC which previously housed single file water was apparently constricted (~28 $Å^2$, Fig. S4) by the close proximities of $\mathbf{B_1}$ and $\mathbf{B_2}$. Instead, a molecule of ethanol was accommodated between $\mathbf{B_2}$ and $\mathbf{B_3}$ to afford BzHAT.EtOH where intramolecular H-bonding between the C=O ($\mathbf{B_3}$) and NH ($\mathbf{B_1}$) was intact (dO···H 2.09 Å) as in IPHAT. We further attempted growing crystals from aqueous methanol (1:1) which on examination turned out to be methanolate (BzHAT.MeOH) where intramolecular H-

bonding between the C=O ($\mathbf{B_3}$) and NH ($\mathbf{B_1}$) deviated by an infinitesimally small difference (dO···H 2.08 Å) when compared with that in BzHAT.EtOH. Both methanolate and ethanolate crystallizes in monoclinic crystal systems, solved and refined in the space group *P2(1)/n* with packing coefficients 0.638 and 0.636 respectively (Fig. S5). The solvent molecules aligned between $\mathbf{B_2}$ and $\mathbf{B_3}$ and enclosed inside a hydrophobic cavity formed by phenyl rings, act as bridge for thiazole dimer formation (Fig. 7) and are forming centro-symmetric hexameric arrangement of solvent molecules with a chair conformation.[86, 87]

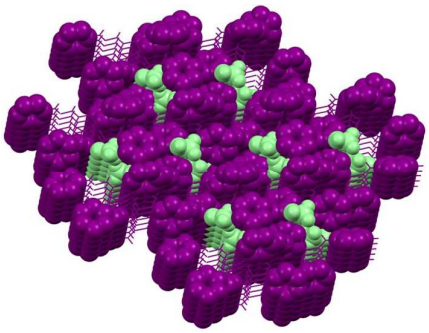

Fig.7 Solvent molecules (light green) enclosed in the hydrophobic cavity formed by phenyl rings in the super structure of BzHAT. Phenyl rings and solvent molecules are CPK representation.

Both methanol and ethanol form two H-bonds in their respective crystals - (i) oxygen atom of solvent acting as acceptor and NH in $\mathbf{B_2}$ (dO···H 1.95 Å in BzHAT.MeOH and 1.91 Å in BzHAT.EtOH) as donor, and (ii) a bifurcated bond where C=O in $\mathbf{B_3}$ as acceptor and OH in solvent as donor at a distance of 1.900 Å and 1.997 Å respectively (Fig. 8) by *cooperative effect*[88] shown by majority of monoalcoholic systems.

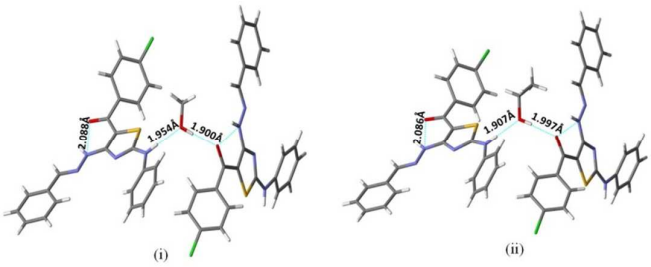

Fig. 8 View of H-bonding interactions (dashed line) of (i) BzHAT.MeOH and (ii) BzHAT.EtOH along *c* axis. Atoms are shown in capped stick representation.

The NRC in the super structures of both methanolate and ethanolate comprise an area of 27-28 $Å^2$ (Fig. S4) and are apparently constricted when compared with that in IPHAT accounting for the absence of water wire. When viewed in the *bc* plane these channels form a *herringbone* type arrangement (interchain separations; 14.844 Å in BzHAT.MeOH and 16.416 Å in BzHAT.EtOH) and along the *ac* plane the molecules are arranged in layers with an inter layer distance of 16.189 Å and 16.416 Å in BzHAT.MeOH and BzAHT-1.EtOH respectively (Fig. 9). The interlayer distance was almost four fold enhanced when compared to that in IPHAT probably due to the bulky solvent molecules.

Journal Name

ARTICLE

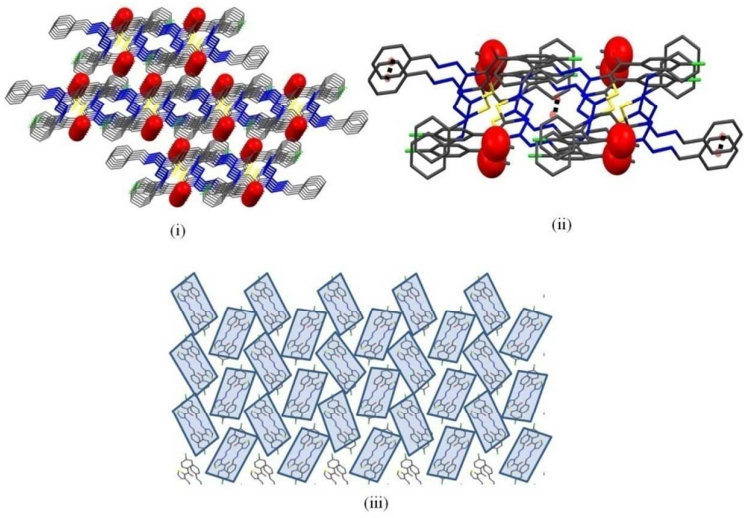

Fig. 9 (i) Supramolecular assembly of BzHAT alcoholates in the *ac* plane. (ii) Distance between adjuscent layers (centroid-centroid) is marked with black dotted line. Oxygen atom of solvent molecule is in CPK representation. All H atoms are omitted for clarity of view. (iii) *Herringbone* arrangement of NRC of BzHAT alcoholates viewed *bc* plane. Solvent molecules are omitted for clarity of view.

The alcoholic oxygen atoms defined a parallel triangular wave symmetry in the *bc* plane with an O-O distance of ~9.7 Å. (9.712 in BzHAT.MeOH and 9.773 in BzHAT.EtOH) (Fig. 10), whereas the S atoms of thiazole rings aligned *anti* to the $\mathbf{B_2}$ NH, formed a regular parallel 'Z' like arrangement in the superstructure (Fig. 11).

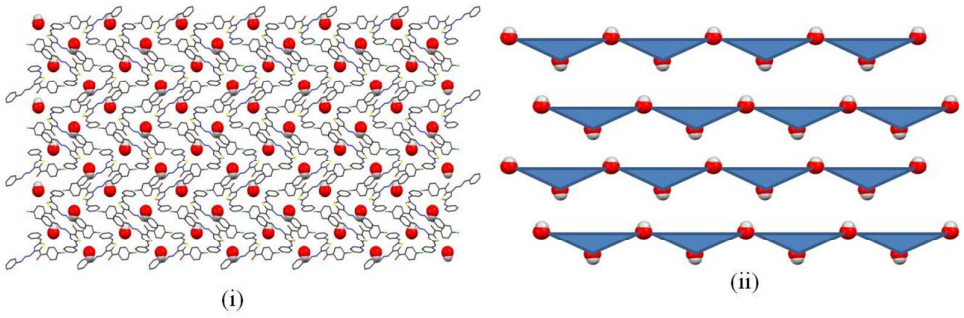

Fig. 10 (i) Molecular packing of BzHAT alcoholate along *bc* plane. Alcoholic O and H are in CPK representation for clarity purpose. (ii) Triangular wave arrangement of solvent molecules in the same plane.

Journal Name

ARTICLE

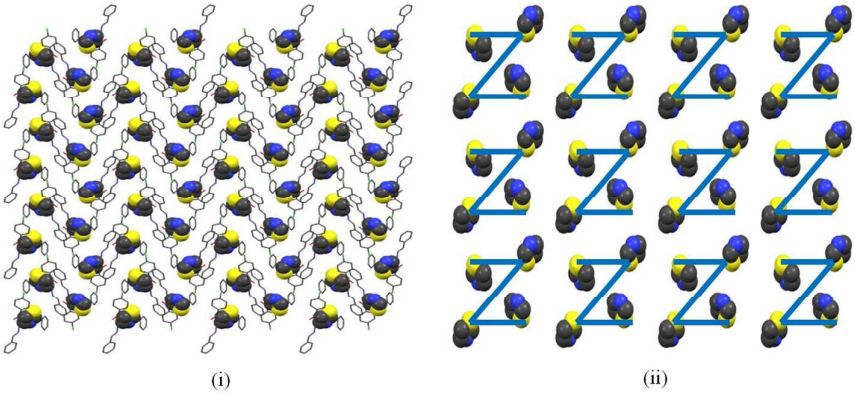

Fig. 11 (i) View of thiazole ring packing of BzHAT along *bc* plane. Thiazole rings are in CPK representation for clarity purpose. (ii) 'Z' like arrangement of thiazole S atoms in the plane.

The variations in channel dimensions and subsequent guest encapsulations substantiate our hypothesis on the probable role of hydrazone substituent on the channel formation and tunability. To further strengthen our hypothesis, a cyclohexyl unit was provided as the hydrazone capping and the variations in channel formations and dimensions were investigated.

Uninhabited channels

Diffraction quality crystals of 4-cyclohexylidene-5-benzoyl-2-phenylamino-1,3-thiazole (CyHAT) from aqueous ethanol (1:1) appeared in triclinic crystal system, solved and refined in the space group *P-1* with a packing coefficient of 1.26. The asymmetric unit of the crystal contains two chemically identical but crystallographically different molecules bonded together by inter molecular H-bonding (Fig. 12) in a graph set $R_2^2(8)$.

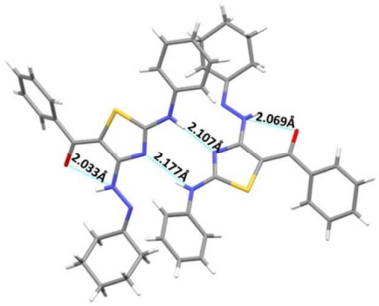

Fig. 12 View of H-bonding interactions (dashed line) in CyHAT along *a* axis. Atoms are shown in capped stick representation.

The thiazole N atoms act as H-bond acceptors whereas the $\mathbf{B_1}$ NH act as H-bond donors (~2.1 Å, dN···H) to orient the rings such that S atoms in the dimeric unit are oppositely aligned to generate a pincer- shaped NRC with thiazole N-N distance of 10.362 Å (Fig. 13). Surprisingly this time there was no water/solvent inclusion in the channels probably due to open structure of the channel and hence establishing the role of NRC.

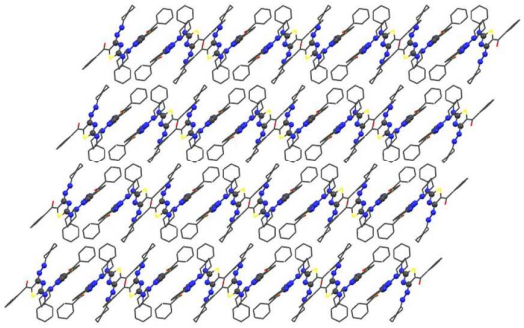

Fig. 13 Pincer-shaped channels of CyHAT viewed along *ac* plane. N and C atoms in the channel are shown in ball and stick representation. All H atoms are omitted for clarity of view.

However, intramolecular H-bonding between the C=O (**B_3**) and NH (**B_1**) was intact and the bond distances (dO···H 2.07 or 2.03 Å) were higher than that in IPHAT derivatives and lower than in BzHAT systems. The molecules are arranged in layers along *ac* plane with an inter layer distance of 12.649 Å and when viewed along *a* axis, shows calixarene type of arrangement in which thiazole rings are facing each other with a S-S distance of 4.218 and 4.630 Å in alternate layers (Fig. 14).

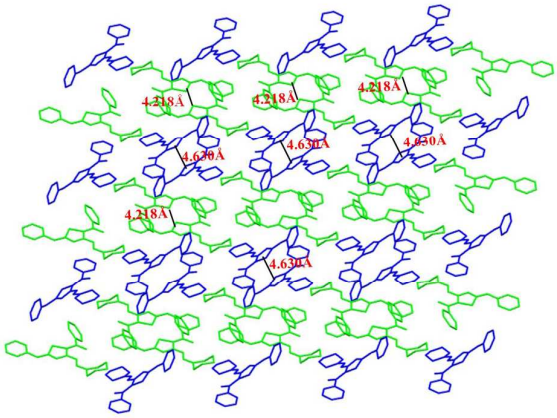

Fig.14 Calixarene type of arrangement of CyHAT along *a* axis. Thiazole S-S distance is marked with a black line. All the atoms are shown in capped stick representation.

Moreover continuous hydrophobic channel formed by the cyclohexane unit in **B_1** and the phenyl ring on **B_3** observed along *c* axis resembled cyclohexane ring in its chair form (Fig. 15) which is most common in organic porous materials.[89] The role of steric factors on the channel formations/dimensions are currently pursued by incorporating substituted cyclohexanones and will appear elsewhere.

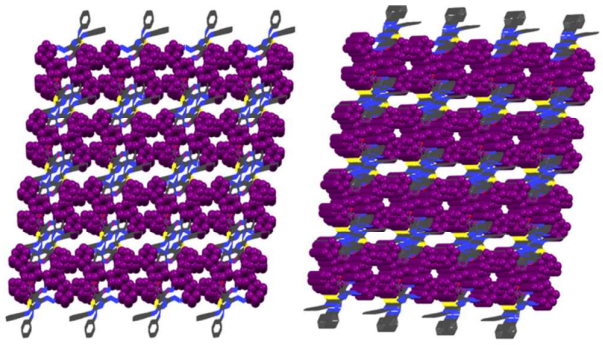

Fig. 15 Views of hydrophobic cavity observed along *c axis* of CyHAT crystal packing. Cyclohexane unit and phenyl ring (purple colour) on **B3** are in CPK representation.

Experimental Section

Materials and Methods

The starting materials phenacyl bromide and 4-chlorophenacyl bromide for synthesis were purchased form Sigma-Aldrich, USA and Spectrochem Ltd., India respectively and were used as received. DMSO and Et_3N were purchased form Merck chemicals. IR spectra were obtained using PerkinElmer Spectrum 100 FT-IR spectrometer using KBr pellets in the 4000-450 cm^{-1} region. NMR spectra were recorded using Bruker AV III 500 MHz FT- NMR spectrometer using $CDCl_3$ as solvent. Chemical Shifts for ^1H and ^{13}C NMR were reported in parts per million (ppm). Mass analysis was obtained using Waters (Micromass) Quattro II spectrometers. The C, H, N elemental analysis was carried out using Perkin-Elmer 2400 Series CHNS/O Analyser.

Synthesis of 5-benzoyl-4-isopropylidenehydrazino-2-phenylaminothiazole (IPHAT 1) *N*-(isopropylideneamino)-*N'*-

(phenylthiocarbamoyl)guanidine (0.125 g, 0.5 mmol) and phenacyl bromide (0.097 g, 0.49 mmol) in DMSO containing Et_3N (1 mmol) were stirred for 5-10 min at room temperature. The reaction mixture was then added to crushed ice and the precipitate formed was filtered off and dried in air. Product obtained was recrystallized with ethanol-acetone (1:1) mixture resulted in yellow fluffy solid. Yield: 0.325 g (93%). M.p.: 206-208 °C. Anal. Calcd. for $C_{19}H_{17}ClN_4OS$: C, 65.12; H, 5.18; N, 15.99%. Found: C, 65.08; H, 5.14; N, 15.83%. IR (KBr): 3220, 3060, 1600, 1580, 1530, 730, 690 cm^{-1}. ^1H NMR (270 MHz; $CDCl_3$): δ 1.96 (3H, s, Me), 2.03 (3H, s, Me), 7.17-7.47 (8H, m, Ph), 7.73-7.46 (2H, m, Ph), 8.97 (1H, s, NH), 12.09 (1H, s, NH). ^{13}C NMR (67.9 MHz; $CDCl_3$): δ 17.0, 24.9, 94.4, 121.2, 125.5, 127.1, 128.3, 129.5, 130.5, 138.3, 141.2, 152.1, 161.8, 171.3, 183.9. EI-MS: m/z 350 (M^+, 41%), 245(6), 119(21), 105(37), 77(100), 56(19).

Synthesis of 4-benzylidenehydrazino-5-(4-chlorobenzoyl)-2-phenylaminothiazole (BzHAT). *N*-(benzylideneamino)-*N'*-(phenylthiocarbamoyl)guanidine (0.125 g, 0.5 mmol)) and 4-chlorophenacyl bromide (0.115 g, 0.49 mmol) in DMSO containing Et_3N (1 mmol) were stirred for 5-10 min at room temperature. The reaction mixture was then added to crushed ice and the precipitate formed was filtered off and dried in air. Product obtained was recrystallized with ethanol-acetone (1:1) mixture resulted in yellow fluffy solid. Yield: 0.397 g (92%). M.p.: 163.1-163.7 °C. IR (KBr): 3480-2870, 1697, 1556, 1352, 1072, 938,788 cm^{-1}. ^1H NMR (270 MHz; $CDCl_3$): δ 7.09 (2H, s, Ph), 7.24-7.41 (8H, m, Ph), 7.57 (2H, s, Ph), 7.70 (2H, s, Ph), 9.78(1H, s, NH), 12.35 (2H, s, NH). ^{13}C NMR (67.9 MHz; $CDCl_3$): δ 94.4, 121.5, 125.9, 127.4, 128.5, 128.7, 129.4, 133.7, 136.9, 138.2, 139.5, 145.8, 161.5, 171.6, 182.9.

X-ray Crystallography

Diffraction data were collected on Bruker Kappa APEX-II single crystal X-ray diffractometer equipped with graphite-monochromated Mo- Kα radiation (λ = 0.71073 Å). Crystallographic details for crystals were collected at T =296 K (IPHAT 1, BzHAT), T = 293K (IPHAT 2) and T = 150 K (CyHAT). Crystal cell constants were calculated by least-squares global refinement. The structures were solved by direct methods using SHELXS and were refined by constrained full least-squares on F^2 with SHELXTL.[90] Graphics were generated using MERCURY 3.3. X-ray crystal analysis software. Diffraction quality crystals of the molecules were obtained from 1:1 aqueous ethanol or methanol by slow evaporation method. Summary of structural data for the molecules is provided in Table 2.

Table 2 Summary of crystallographic data and structure refinement summary for compounds.

Journal Name

ARTICLE

Compound	IPHAT 1	IPHAT 2	BzHAT.MeOH	BzHAT.EtOH	CyHAT
Empirical formula	$C_{19}H_{20}N_4O_2S$	$C_{19}H_{19}ClN_4O_2S$	$C_{24}H_{21}ClN_4O_2S$	$C_{25}H_{23}ClN_4O_2S$	$C_{22}H_{22}N_4OS$
Formula weight	368.45	402.89	464.96	478.98	390.49
Space group	$P2_1/c$	$P2_1/c$	$P2(1)/n$	$P2(1)/n$	$P\text{-}1$
Crystal system	Monoclinic	Monoclinic	Monoclinic	Monoclinic	Triclinic
T/K	296(2)	293(2)	296(2)	296(2)	150(2)
Crystal dimensions (mm)	0.25 x 0.20 x 0.15	0.30 x 0.20 x 0.20	0.25 x 0.20 x 0.20	0.25 x 0.20 x 0.15	0.50 x 0.15 x 0.15
a/Å	14.450(5)	14.8580(5)	9.6388(3)	9.6720(2)	11.987(16)
b/Å	4.956(5)	4.85400(10)	16.1889(4)	16.4163(3)	12.649(16)
c/Å	26.730(5)	26.8190(8)	14.8442(5)	15.2160(3)	14.39(2)
α (^{0})	90	90	90	90	102.66(3)
β (^{0})	96.301(5)	90.2370(10)	91.0760(10)	90.8050(10)	106.82(2)
γ (^{0})	90	90	90	90	93.196(12)
V/Å^3	1903(2)	1934.19(10)	2315.90(12)	2415.73(8)	2021(5)
ρ_{cald}	1.286	1.384	1.334	1.317	1.283
Z	4	4	4	4	4
λ (Å)	0.71073	0.71073	0.71073	0.71073	0.71073
Goodness-of-fit	1.040	1.025	1.036	1.043	0.605
R_1 (all data)	0.0925	0.0612	0.0421	0.0612	0.1780
wR_2 [for I>2σ(I)]	0.1823	0.1098	0.0897	0.1136	0.1079
Reflections collected	12965	13987	17752	20680	8003
Independent reflection	3335	3394	4084	5259	1748

Journal Name

ARTICLE

Conclusions

In conclusion, crystal landscapes in propeller shaped trivariant systems with thiazole hub and tunable blades B1-B3 revealed the critical role of the carbonyl variant in the supramolecular assemblies. Focusing on the B1 variant, nitrogen rich channels (NRC) with varying dimensions and guest encapsulations were generated. The NRC formed by isopropylidene capped hydrazinothiazole adopted a left handed helical conformation inside which single file water was stabilized, and could serve as a synthetic model of water/proton transport for helical membrane proteins stabilizing 1D water chains. Benzylidene units contributed to constriction of NRC and located a centro-symmetric hexameric arrangement of polar protic solvent molecules with a chair conformation outside the channel, whereas cyclohexylidene unit imparted a pincer-shape to the channel devoid of guest molecules. We expect these unique and unexplored class of thiazole based scaffolds with their inherently multiplied diversity to reveal much more assorted structural landscapes and demonstrate their potential in varied applications. .

Acknowledgements

(ST acknowledges IIST for financial assistance. We thank SAIF, IIT-M, IISER, Thiruvananthapuram and NIIST, Thiruvananthapuram for the spectral data and single crystal XRD measurements.

Notes and references

Synthesis characterization of IPHAT 2 and CyHAT were published earlier.

1. G. R. Desiraju, *Angew. Chem., Int. Ed. Engl.* , 1995, **34**, 2311.
2. B. Moulton and M. J. Zaworotko, *Chem. Rev.*, 2001, **101**, 1629.
3. A. C. Anderson, *Chem. Biol.* , 2003, **10**, 787.
4. K. A. Thiel, *Nature Biotechnol.* , 2004, **22**, 513.
5. S. Datta and D. J. Grant, *Nature Rev. Drug Discov.*, 2004, **3**, 42.
6. S. L. Schreiber, *Science*, 2000, **287**, 1964.
7. M. D. Burke, E. M. Berger and S. L. Schreiber, *Science*, 2003, **302**, 613.
8. W. H. Sauer and M. K. Schwarz, *J. Chem. Inf. Comput. Sci.* , 2003, **43**, 987.
9. M. D. Burke and S. L. Schreiber, *Angew. Chem., Int. Ed. Engl.*, 2004, **43**, 46.
10. J. J. Perez, *Chem. Soc. Rev.*, 2005, **34**, 143.
11. S. L. Schreiber, *Nature*, 2009, **457**, 153.
12. G. R. Desiraju and G. W. Parshall, *Mater. Sci. Monogr.*, 1989, **54**.
13. G. A. Jeffrey, *An introduction to hydrogen bonding*, Oxford university press New York, 1997.
14. C. B. Aakeröy, N. R. Champness and C. Janiak, *Cryst. Eng. Comm.*, 2010, **12**, 22.
15. A. Delori, P. T. Galek, E. Pidcock and W. Jones, *Chem. Eur. J.*, 2012, **18**, 6835.
16. A. Alex, D. S. Millan, M. Perez, F. Wakenhut and G. A. Whitlock, *Med. Chem. Comm.*, 2011, **2**, 669.
17. G. R. Desiraju and T. Steiner, *Weak hydrogen bond*, Oxford University Press New York, 2001.
18. G. R. Desiraju, *Angew. Chem. Int. Ed. Engl.* , 2007, **46**, 8342.
19. G. R. Desiraju, ed., *Crystal engineering. Structure and function. Perspectives in supramolecular chemistry*, Chichester: Wiley, 2003.
20. S. Sengupta, S. L. Smitha, N. E. Thomas, T. R. Santhoshkumar, S. K. Devi, K. G. Sreejalekshmi and K. N. Rajasekharan, *Br. J. Pharmacol.* , 2005, **145**, 1076.
21. K. G. Sreejalekshmi, S. K. Devi and K. N. Rajasekharan, *Tet. Lett.* , 2006, **47**, 6179.
22. K. G. Sreejalekshmi and K. N. Rajasekharan, *Tet. Lett.*, 2012, **53**, 3627.
23. D. Cook, D. Brown, R. Alexander, R. March, P. Morgan, G. Satterthwaite and M. N. Pangalos, *Nature Rev. Drug Discov.* , 2014. **13**, 419.
24. F. Pammolli, L. Magazzini and M. Riccaboni, *Nature Rev. Drug Discov.*, 2011, **10**, 428.
25. B. Munos, *Nature Rev. Drug Discov.*, 2009, **8**, 959.
26. S. M. Paul, D. S. Mytelka, C. T. Dunwiddie, C. C. Persinger, B. H. Munos, S. R. Lindborg and A. L. Schacht, *Nature Rev. Drug Discov.*, 2010, **9**, 203.
27. J. W. Scannell, A. Blanckley, H. Boldon and B. Warrington, *Nature Rev. Drug Discov.*, 2012, **11**, 191.
28. Ö. Almarsson and M. J. Zaworotko, *Chem. Commun.* , 2004, 1889.
29. P. Vishweshwar, J. A. Mcmahon, J. A. Bis and M. J. Zaworotko, *J. Pharm. Sci.* , 2006, **95**, 499.
30. A. V. Trask, *Mol. Pharm.* , 2007, **4**, 301.
31. N. Shan and M. J. Zaworotko, *Drug Discov. Today*, 2008, **13**, 440.
32. D. J. Good and N. r. Rodríguez-Hornedo, *Cryst. Growth Des.* , 2009, **9**, 2252.
33. S. Titus and K. G. Sreejalekshmi, *Tet. Lett.*, 2014, **55**, 5465.
34. G. R. Desiraju, *Chem. Soc. Chem. Commun.* , 1991, 426.
35. A. D. Bond, *Cryst. Eng. Comm.*, 2007, **9**, 833.

36. M. Chaplin, *Nature Rev. Mol. Cell Biol.*, 2006, **7**, 861.
37. P. Ball, *Chem. Rev.* , 2008, **108**, 74.
38. M. Barboiu, *Angew. Chem. Int. Ed.*, 2012, **51**, 11674.
39. H. Zhao, S. Sheng, Y. Hong and H. Zeng, *J. Am. Chem. Soc.*, 2014, **136**, 14270.
40. C. Moon, G. M. Preston, C. A. Griffin, E. W. Jabs and P. Agre, *J. Biol. Chem.*, 1993, **268**, 15772.
41. H. Sui, B.-G. Han, J. K. Lee, P. Walian and B. K. Jap, *Nature*, 2001, **414**, 872.
42. D. Kozono, M. Yasui, L. S. King and P. Agre, *J. Clin. Invest.*, 2002, **109**, 1395.
43. E. Tajkhorshid, P. Nollert, M. Ø. Jensen, L. J. Miercke, J. O'Connell, R. M. Stroud and K. Schulten, *Science*, 2002, **296**, 525.
44. U. K. Eriksson, G. Fischer, R. Friemann, G. Enkavi, E. Tajkhorshid and R. Neutze, *Science*, 2013, **340**, 1346.
45. S. Gravelle, L. Joly, F. Detcheverry, C. Ybert, C. Cottin-Bizonne and L. Bocquet, *Proc. Natl. Acad. Sci.* , 2013, **110**, 16367.
46. M. Akeson and D. W. Deamer, *Biophys. J.*, 1991, **60**, 101.
47. G. A. Woolley and B. Wallace, *J. Membr. Biol.*, 1992, **129**, 109.
48. A. Chernyshev, K. M. Armstrong and S. Cukierman, *Biophys. J.*, 2003, **84**, 238.
49. D. A. Kelkar and A. Chattopadhyay, *Biochimica et Biophysica Acta (BBA)-Biomembranes*, 2007, **1768**, 2011.
50. H. D. Song and T. L. Beck, *J. Phys. Chem. C*, 2013, **117**, 3701.
51. J. A. Kornblatt, *Biophys. J.*, 1998, **75**, 3127.
52. M. Wikström, M. I. Verkhovsky and G. Hummer, *Biochimica et Biophysica Acta (BBA)-Bioenergetics*, 2003, **1604**, 61.
53. M. Wikström, *Biochimica et Biophysica Acta (BBA)-Bioenergetics*, 2004, **1655**, 241.
54. I. Belevich, M. I. Verkhovsky and M. Wikström, *Nature*, 2006, **440**, 829.
55. V. R. Kaila, M. I. Verkhovsky and M. Wikström, *Chem. Rev.*, 2010, **110**, 7062.
56. V. Sharma, G. Enkavi, I. Vattulainen, T. Róg and M. Wikström, *Proc. Natl. Acad. Sci.* , 2015, **112**, 2040.
57. A.-N. Bondar, S. Fischer and J. C. Smith, *J. Membr. Biol.*, 2011, **239**, 73.
58. N. J. Claassens, M. Volpers, V. A. M. dos Santos, J. van der Oost and W. M. de Vos, *Trends Biotechnol.*, 2013, **31**, 633.
59. K. Gerwert, E. Freier and S. Wolf, *Biochimica et Biophysica Acta (BBA)-Bioenergetics*, 2014, **1837**, 606.
60. Y. Levy and J. N. Onuchic, *Annu. Rev. Biophys. Biomol. Struct.*, 2006, **35**, 389.
61. D. Thirumalai, G. Reddy and J. E. Straub, *Acc. Chem. Res.*, 2011, **45**, 83.
62. S. Yuan, S. Filipek, K. Palczewski and H. Vogel, *Nature Commun.*, 2014, **5**.
63. M. Barboiu and A. Gilles, *Acc. Chem. Res.*, 2013, **46**, 2814.
64. P. Agre, L. S. King, M. Yasui, W. B. Guggino, O. P. Ottersen, Y. Fujiyoshi, A. Engel and S. Nielsen, *J. Physiol.*, 2002, **542**, 3.
65. P. Agre, *Angew. Chem., Int. Ed. Engl.* , 2004, **43**, 4278.
66. L. H. Pinto, G. R. Dieckmann, C. S. Gandhi, C. G. Papworth, J. Braman, M. A. Shaughnessy, J. D. Lear, R. A. Lamb and W. F. DeGrado, *Proc. Natl. Acad. Sci.* , 1997, **94**, 11301.
67. J. R. Schnell and J. J. Chou, *Nature*, 2008, **451**, 591.
68. M. D. Hollingsworth, *Science*, 2002, **295**, 2410.
69. M. Mascal, L. Infantes and J. Chisholm, *Angew. Chem., Int. Ed. Engl.* , 2006, **45**, 32.
70. G. R. Desiraju, *Angew. Chem., Int. Ed. Engl.* , 2007, **46**, 8342.
71. M. Amorín, A. L. Llamas-Saiz, L. Castedo and J. R. Granja, *Cryst. Growth Des.*, 2011, **11**, 3351.
72. G. R. Desiraju, J. J. Vittal and A. Ramanan, *Crystal engineering: a textbook*, World Scientific, 2011.
73. R. Natarajan, L. Bridgland, A. Sirikulkajorn, J.-H. Lee, M. F. Haddow, G. Magro, B. Ali, S. Narayanan, P. Strickland and J. P. Charmant, *J. Am. Chem. Soc.*, 2013, **135**, 16912.
74. Y.-T. Wang, G.-M. Tang, J.-H. Wang, W.-Z. Wan, T.-X. Qin, Y.-Q. Wang, K.-L. Mou, T.-D. Li and L.-F. Ma, *Cryst. Eng. Comm.*, 2013, **15**, 7430.
75. L. Infantes, L. Fábián and W. S. Motherwell, *Cryst. Eng. Comm.*, 2007, **9**, 65.
76. D. R. Turner, M. J. Paterson and J. W. Steed, *J. Org. Chem.*, 2006, **71**, 1598.
77. L. Ma, W. A. Harrell Jr and J. T. Davis, *Org. Lett.*, 2009, **11**, 1599.
78. M. N. Hoque, A. Basu and G. Das, *Cryst. Growth Des.*, 2013, **14**, 6.
79. L. E. Cheruzel, M. S. Pometun, M. R. Cecil, M. S. Mashuta, R. J. Wittebort and R. M. Buchanan, *Angew. Chem., Int. Ed. Engl.* , 2003, **115**, 5610.
80. Y. Le Duc, M. Michau, A. Gilles, V. Gence, Y. M. Legrand, A. van der Lee, S. Tingry and M. Barboiu, *Angew. Chem., Int. Ed. Engl.* , 2011, **123**, 11568.
81. B. S. Kumar and P. K. Panda, *Cryst. Eng. Comm.*, 2014, **16**, 8669.
82. N. J. Babu and A. Nangia, *Cryst. Growth Des.*, 2006, **6**, 1995.
83. S. Varughese and G. R. Desiraju, *Cryst. Growth Des.*, 2010, **10**, 4184.
84. M. C. Etter, *Acc. Chem. Res.*, 1990, **23**, 120.
85. P. Aryal, M. S. Sansom and S. J. Tucker, *J. Mol. Biol.*, 2015, **427**, 121.
86. M. Arunachalam, E. Suresh and P. Ghosh, *Tet. Lett.*, 2007, **48**, 2909.
87. M. A. Little, M. E. Briggs, J. T. Jones, M. Schmidtmann, T. Hasell, S. Y. Chong, K. E. Jelfs, L. Chen and A. I. Cooper, *Nat. Chem.*, 2015, **7**, 153.
88. C. Ceccarelli, G. Jeffrey and R. Taylor, *J. Mol. Struct.*, 1981, **70**, 255.
89. J. Tian, P. K. Thallapally and B. P. McGrail, *Cryst. Eng. Comm.*, 2012, **14**, 1909.
90. G. M. Sheldrick, SHELXL-2013, Gӧttingen University: Germany, 2014.

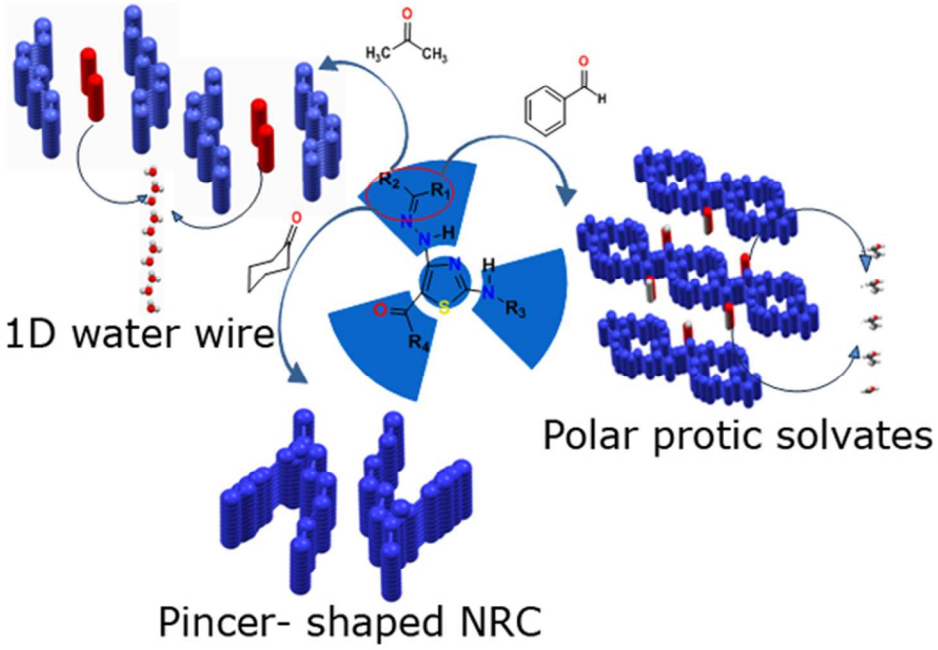

59x39mm (300 x 300 DPI)